EXPERIMENTAL STUDY ON SEISMIC BEHAVIOR OF REINFORCED FULLY GROUTED CONCRETE MASONRY WALLS

Kenji KIKUCHI [1], Koji YOSHIMURA [2] and Akihiro TANAKA [3]

SUMMARY

Reinforced fully-grouted concrete masonry (grouted masonry) walls are composed of hollow concrete masonry units, vertical and horizontal reinforcing-bars and cast-in-place grouting concrete. The presence of hollow concrete masonry units, which are one of the principal materials in grouted masonry walls, has a large effect on the seismic behavior of the grouted masonry walls. Main objective of the present study is to investigate this effect experimentally. Eight different bearing wall specimens, including grouted masonry walls and reinforced concrete (R/C) walls, are tested under constant vertical axial loads and alternately repeated lateral forces. The amount of vertical and horizontal reinforcement is the other experimental parameter. The test results indicate that the masonry units in the grouted masonry walls can effectively carry lateral loads in the walls as well as grouted concrete and the grouted masonry walls have almost the same seismic resistant capacity as the R/C walls. In addition, the accuracy of the predicted ultimate flexural and shear strengths of the grouted masonry walls by the existing equations are verified in this paper.

1. INTRODUCTION

Reinforced fully-grouted concrete masonry building system is one of the boxed-wall structures, which is composed of grouted masonry walls, R/C wall girder and horizontal floor slab as shown in Figure 1, and are expected to be widely used in future in Japan, because there was almost no structural damage to this type of masonry buildings during the 1995 Hyogoken-nanbu (Kobe) earthquake [Bruneau et al., 1996]. Two different standards of the AIJ (Architectural Institute of Japan) are available to structural design of the grouted masonry buildings. One is the Standard for low-rise (up to three stories) buildings which was established in 1952 and the latest version was revised in 1997 [AIJ, 1994 and AIJ, 1997]. The other is the Standard for medium-rise (four or five stories) buildings which was newly published in late 1997 [Yoshimura et al., 1997 and AIJ, 1997]. In

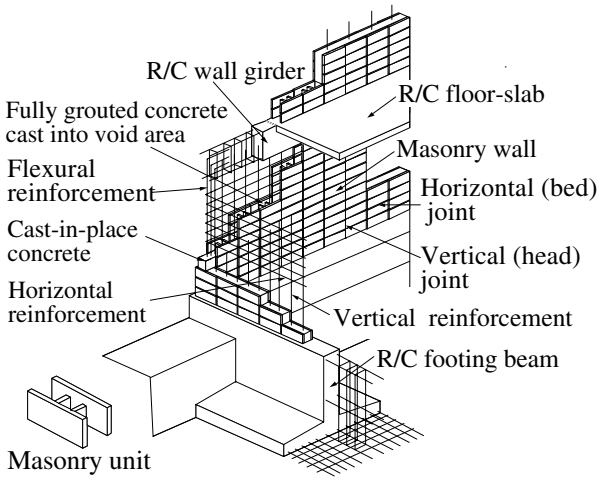

Figure 1: A typical reinforced fully-grouted concrete masonry building

[1] *Department of Architectural Engineering, Oita University, Oita, Japan*
Email: kikuchi@cc.oita-u.ac.jp

[2] *Department of Architectural Engineering, Oita University, Oita, Japan*
Email: kojiysmr@cc.oita-u.ac.jp

[3] *Umebayashi Construction Co., Ltd., Oita and Department of Architectural Engineering, Oita University, Oita, Japan*
Email: atanaka@arch.oita-u.ac.jp

order to develop much more seismic medium-rise reinforced fully-grouted concrete masonry buildings, it is very important to investigate the seismic behavior of grouted masonry walls under severe earthquake loading. The presence of hollow concrete masonry units, which is one of the principal materials in grouted masonry walls, has a large effect on the seismic behavior of grouted masonry walls such as initial stiffness, ultimate strength and failure mode. Up to the present time, however, there are quite few studies focusing on this effect [Kaminosono et al., 1985].

The main objective of the present study is to examine the effect of the presence of masonry units on the seismic behavior of grouted masonry walls experimentally. Eight different bearing wall specimens, including grouted masonry walls and R/C walls, were designed and constructed. In addition, the amount of vertical and horizontal reinforcement was also adopted as an experimental parameter. All the specimens were tested under the condition of constant vertical axial load and alternately repeated lateral forces. Based on the results obtained from the eight different test specimens, the effect of face shells and webs of the masonry units on the seismic behavior of grouted masonry wall is discussed. In addition, the accuracy of the predicted ultimate flexural and shear strengths of the grouted masonry walls by the existing equations in Japan are verified by using the test results of ten different bearing wall specimens including four specimens in the previous test series conducted by the authors [Kikuchi et al., 1997].

2. TEST SPECIMENS

Eight different bearing wall specimens shown in Figure 2 and listed in Table 1 were designed and constructed. Size and shape of the hollow concrete masonry unit used for the grouted masonry walls is shown in Figure 3. All the specimens are approximately one-half scale models of one-story slender bearing walls. Horizontal lengths (l) and clear height (h_0) of the wall panel are 79 cm and 120 cm, and total height of the bearing wall is 150 cm including the depth of cast-in-place wall girder at top of each wall. Width of horizontal and vertical mortar joints in the grouted masonry walls is 1.0 cm. Walls of the test specimens are classified into four types; that is, (a) GM type; grouted masonry walls having 19 cm thickness, (b) RC-190 type; R/C walls

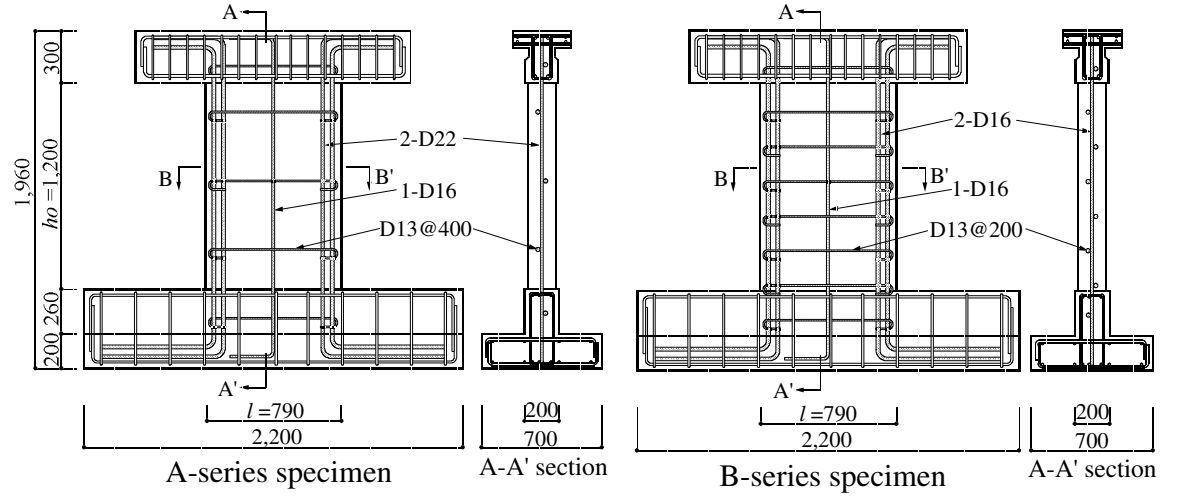

Specimen type	GM	RC-190	RC-125	GM-F
B-B' Section	Masonry unit, 190, 790	190, 790	125, 790	Web, 125, 790
Elevation of wall panels	Face shells, Mortar joints, Triaxial strain gage	Triaxial strain gage	Triaxial strain gage	Webs, Triaxial strain gage

(Unit in mm)

Figure 2: Size and shape, and reinforcement of test specimens

having the same thickness (19 cm) as the grouted masonry wall, (c) RC-125 type; R/C walls having the same thickness (12.5 cm) as grouted concrete in the wall, and (d) GM-F type; grouted masonry walls from which all of the face shells of masonry units were removed before testing. All the eight specimens are classified into two test series, that is A-series and B-series, depending on the amount of vertical and horizontal reinforcement. As shown in Figure 2, A-series specimens have longitudinal flexural reinforcing bars (rebars) with bar-size of 2-D22 (or #7), a vertical rebar with bar-size of 1-D16 (or #5), and horizontal rebars with bar-size of D13 (or #4), spacing of which is 400 mm. B-series specimens have the longitudinal flexural rebars with bar-size of 2-D16 (or #5), the vertical rebar with bar-size of 1-D16 (or #5), and the horizontal rebars with bar-size of D13 (or #4), spacing of which is 200 mm.

Mechanical properties of materials used for the specimens are shown in Table 2 and Table 3. It is noted that, in case of prisms for GM-F type specimens, all of the face shells of masonry units were removed from the prisms before testing in the same method as the wall panels of GM-F type specimens.

Table 1: List of specimens

Specimens		Wall thickness t (cm)	Flexural rebars $<a_t\ (cm^2)>$	p_t (%)*2	Horizontal rebars	p_{wh} (%)*3	Vertical axial load P (kN)	Vertical axial stress σ_0 (MPa)
A-series specimens	A-GM	19.0	2-D22 <7.74>	0.52	D13 @400	0.17	118	0.78
	A-RC-190							
	A-RC-125	12.5		0.78		0.25		1.19
	A-GM-F *1							
B-series specimens	B-GM	19.0	2-D16 <3.98>	0.27	D13 @200	0.33		0.78
	B-RC-190							
	B-RC-125	12.5		0.40		0.51		1.19
	B-GM-F *1							

[Remarks] *1 All of the face shells of masonry units were removed before testing.
*2 p_t = flexural reinforcement ratio = $a_t / t\ l$,
where a_t = cross-sectional area of flexural rebars, l = wall length, t = wall thickness
*3 p_{wh} = shear reinforcement ratio in horizontal direction = $a_{wh} / t\ h_0$,
where a_{wh} = cross-sectional area of all horizontal rebars, t = wall thickness,
h_0 = clear height of wall

Table 2: Compressive strengths of concrete, mortar, unit and prism

Specimens		Concrete (MPa)	Joint mortar (MPa)	Masonry unit (MPa) (per net section)	Prism (MPa)
A-series specimens	A-GM	34.0	45.8	50.8	33.4
	A-RC-190	32.4	-	-	-
	A-RC-125	34.3	-	-	-
	A-GM-F	32.9	45.8	50.8	23.4
B-series specimens	B-GM	33.0	48.7	50.8	29.2
	B-RC-190	32.4	-	-	-
	B-RC-125	31.3	-	-	-
	B-GM-F	31.8	48.7	50.8	26.7

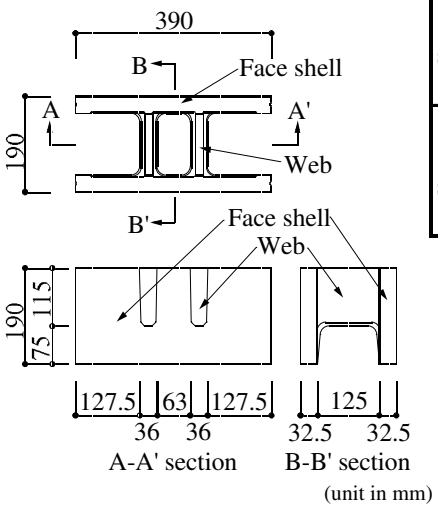

Figure 3: Size and shape of masonry unit

Table 3: Mechanical property of reinforcing bars

Specimens	Rebars	Yield strength (MPa)	Tensile strength (MPa)	Elongation (%)
A-series specimens	D22 (#7)	373	547	24
	D16 (#5)	367	547	22
	D13 (#4)	351	488	21
B-series specimens	D16 (#5)	353	504	20
	D13 (#4)	347	496	15

3. TEST SETUP AND LOADING METHOD

Test setup adopted in the tests is shown in Figure 4. Height of the longitudinal axis of applied lateral forces is 0.55 of the clear height (h_0) of the wall panel measured from the bottom of the wall. Constant axial loads (P=118 kN (12.0 tf)) were applied by a hydraulic jack with the capacity of 490 kN (50 tf), and alternately repeated lateral forces were applied by a double-acting hydraulic jack with 980 kN (100 tf) capacity. Corresponding constant gravity loads applied to the specimens with wall thickness of 19 cm (GM and RC-190 type specimens) and the specimens with wall thickness of 12.5 cm (GM-F and RC-125 type specimens) were σ_0 =0.78 MPa (8.0 kgf/cm^2) and 1.19 MPa (12.2 kgf/cm^2) per gross horizontal area of the bearing wall, respectively. An auxiliary jack installed between loading-beam and reaction-frame is for counterbalancing and setting the test specimens. Important displacements and strains in reinforcing bars and on the surface of the walls were measured by transducers and strain gages and processed simultaneously by a personal computer.

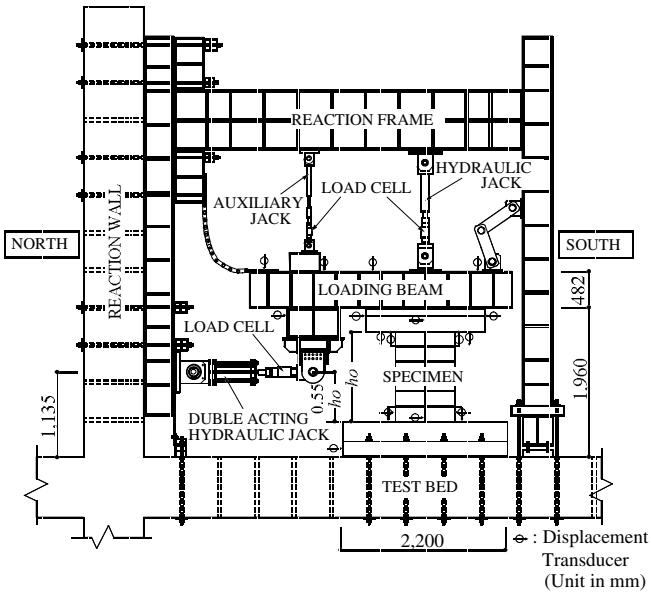

Figure 4: Test setup

4. TEST RESULTS AND DISCUSSIONS

4.1 General Observations

Complete hysteresis loops between applied lateral force (Q) versus story drift (R) relations obtained from all the specimens of A- and B-series tests are shown in Figures 5 (a) through 5 (h), where story drift (R) is defined as the interstory displacement divided by the story-height of the specimen. Dashed lines in the figures represent the ultimate lateral strengths (Q_{mu}) determined by the theoretical ultimate flexural moment capacity at the bottom of each wall, while dotted lines are the theoretical ultimate lateral strengths (Q_{su}) determined by shear failure mode of the bearing wall. All the A-series specimens, where a small amount of shear reinforcement is provided in the

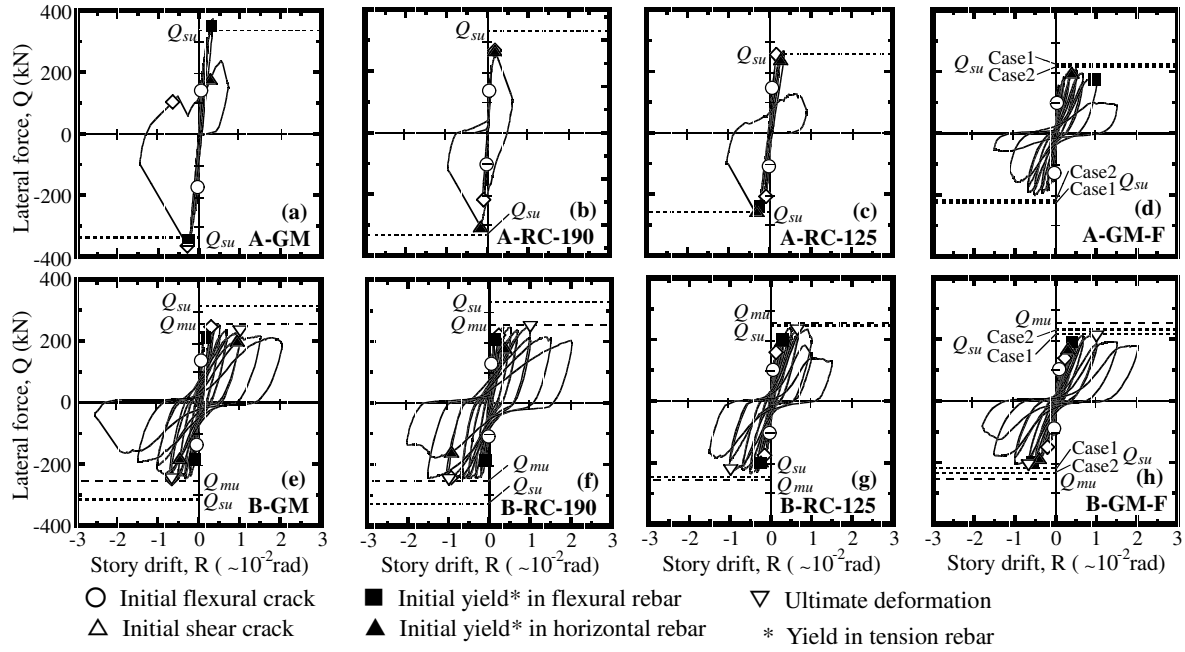

Figure 5: Q-R curves obtained from the test

walls, failed in brittle shear failure mode and then rapid deterioration in lateral load-carrying capacity occurred. On the other hand, specimens B-GM and B-RC-190 in B-series test developed their ultimate lateral strengths in flexure mode and then failed in shear failure mode at R= 1.5×10^{-2} to 2.0×10^{-2} rad. Specimen B-RC-125 failed in flexural failure mode and shear failure mode at almost the same story drift. Specimen B-GM-F failed in shear failure mode.

Final crack patterns observed on the West surfaces of all the specimens of A-series test are shown in Figures 6. A large number of cracks were observed on the surfaces of the GM-F type specimens where webs of the masonry units separated from the face shells are located in the R/C walls. On the contrary, crack patterns observed on the surfaces of the GM type specimens were almost the same as the RC-190 type specimens.

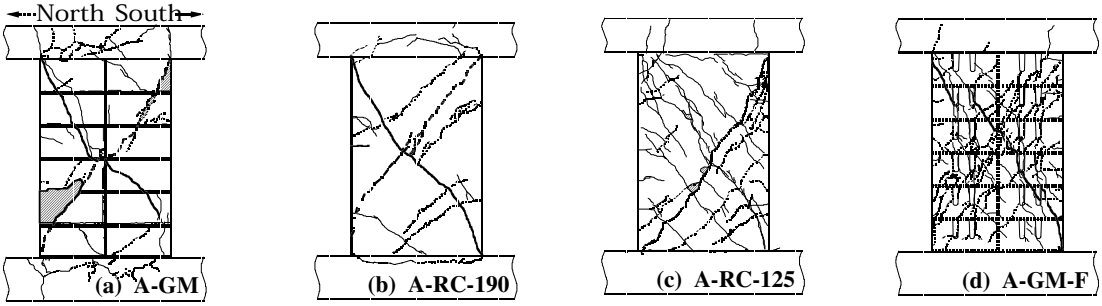

Figure 6: Final crack patterns

4.2 Comparison of Q-R Envelope Curves

Q-R envelope curves obtained from all the Q-R hysteresis loops for A- and B-series specimens are shown in Figures 7 (a) and 7 (b), where lateral forces (Q) are given by the simple average calculated from the North to South- and South to North-side loading curves. Ultimate lateral strengths carried by the GM type specimens (A-GM and B-GM) are higher than those of the RC-125 and GM-F type specimens in the corresponding series test. The specimen A-GM also developed higher ultimate lateral strength than specimen A-RC-190, while that of the specimen B-GM is almost the same as the specimen B-RC-190. These facts mean that the masonry units in the grouted masonry walls can effectively carry lateral loads in the walls as well as the grouted concrete and the grouted masonry walls have almost the same load carrying capacity as the R/C walls. In both A- and B-series tests, ultimate lateral strengths carried by GM-F type specimens are lower than RC-125 type specimens. It can be understood from this result that, in case when the webs of masonry units separated from face shells are located in the R/C walls, the presence of webs reduces the ultimate lateral strengths of the walls. B-series specimens can develop better ductility or deformability than A-series specimens, because the amount of shear reinforcement in B-series specimens is larger than A-series specimens and B-series specimens except for B-GM-F developed their ultimate flexural moment capacities of the wall. In GM-F type specimens, lateral loading capacities decreased slowly after developing their ultimate lateral strengths.

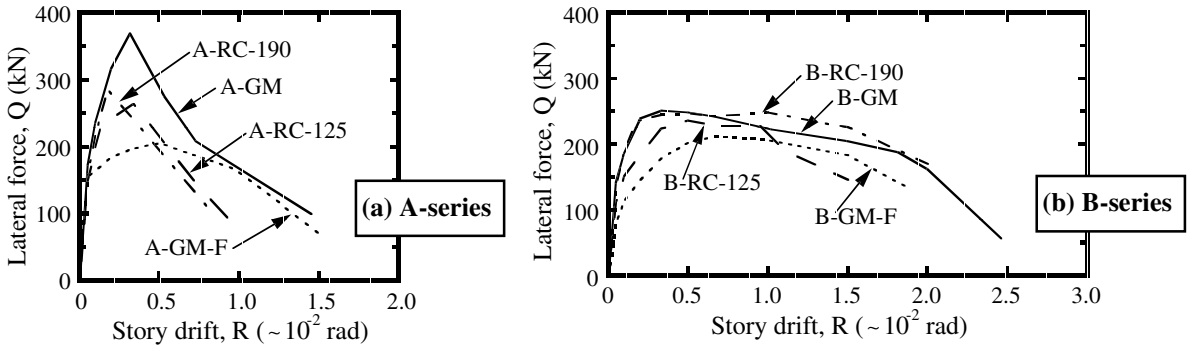

Figure 7: Q-R envelope curves

4.3 Ultimate Lateral Strengths

For all of the A- and B-series specimens, ultimate lateral strengths (Q_{max}) and failure modes observed in their ultimate states are shown in Table 4 together with the theoretical ultimate lateral strengths in flexure mode (Q_{mu}) and shear failure mode (Q_{su}), which are determined by using the existing equations to predict the ultimate flexural and shear strengths of the masonry walls or R/C walls in Japan. It is noted that Equations (1) and (2) (Equations (3.3) and (3.4) in Reference [AIJ, 1990]) were adopted herein to predict the ultimate shear strength (Q_{su}) and ultimate flexural

Table 4: Observed and predicted ultimate lateral strengths and failure modes

Specimens		Theoretical prediction: Ultimate lateral strengths Q_{mu} *1 (kN)	Theoretical prediction: Ultimate lateral strengths Q_{su} *2 (kN)	Theoretical prediction: Expected failure mode *3	Test results: Ultimate lateral strengths Q_{max} (kN): North to south loading	Test results: Ultimate lateral strengths Q_{max} (kN): South to north loading	Test results: Observed failure mode *3	$\frac{Q_{su}}{Q_{mu}}$	$\frac{Q_{max}}{Q_{mu}}$	$\frac{Q_{max}}{Q_{su}}$
A-series specimens	A-GM	417	337	S	375	364	S	0.81	0.90	1.11
	A-RC-190		332	S	268	304	S	0.80	0.64	0.81
	A-RC-125		257	S	267	260	S	0.62	0.64	1.04
	A-GM-F		Case1 *4 220	S	209	202	S	0.53	0.50	0.95
			Case2 *5 218					0.52		0.96
B-series specimens	B-GM	254	315	F	255	247	F S	1.24	1.00	0.81
	B-RC-190		328	F	248	248	F S	1.29	0.98	0.76
	B-RC-125		247	S or F	237	233	FS	0.97	0.93	0.96
	B-GM-F		Case1 *4 219	S or F	214	209	S	0.86	0.84	0.98
			Case2 *5 232					0.91		0.92
H-series *6 specimens	H2-C8	130	192	F	125	120	F	1.47	0.96	0.65
	H1-C8	134	194	F	129	123	F	1.45	0.97	0.67
L-series *6 specimens	L2-C8	328	291	S or F	308	286	F S	0.89	0.94	1.06
	L1-C8	337	321	S or F	334	303	FS	0.95	0.99	1.04

[Remarks] *1 Q_{mu} : Ultimate lateral strength in flexure mode *2 Q_{su} : Ultimate lateral strength in shear failure mode
*3 F : Flexural failure mode, S : Shear failure mode *4 Case 1 : In case of R/C wall having 10.3 cm thickness
*5 Case 2 : In case of grouted masonry wall having 12.5 cm thickness
*6 Grouted masonry wall specimens presented in Reference [Kikuchi, 1997]

strength (M_u) of the reinforced fully-grouted concrete masonry walls, respectively. On the other hand, ultimate strengths (M_u and Q_{su}) of the R/C walls were predicted by Equations (4.5) and (4.6) in Reference [AIJ, 1990].

$$M_u = a_t \cdot \sigma_y \cdot l_w + 0.5 a_w \cdot \sigma_{wy} \cdot l_w + 0.5 N \cdot l_w \qquad (1)$$

where, a_t : cross-sectional area of flexural rebars, σ_y : yield strength of flexural rebars
l_w : 0.9 l, where l : horizontal length of wall, a_w : cross-sectional area of vertical rebars
σ_{wy} : yield strength of vertical rebar, N : axial load of wall

$$Q_{su} = \left\{ \frac{0.053 p_t^{0.23} (F_m + 180)}{M/(Qd) + 0.12} + 2.7\sqrt{\sigma_{wh} \cdot p_{wh}} + 0.1\sigma_0 \right\} t \cdot j \qquad (2)$$

where, p_t : flexural reinforcement ratio = $a_t / t\,l$, in %
F_m : compressive strength of fully grouted masonry by the prism test, in kgf/cm^2
M, Q : maximum design bending moment of wall, in kgf $\cdot$ cm and maximum design shear force of wall, in kgf
d : effective depth of wall, in cm, σ_{wh} : yield strength of horizontal shear rebar, in kgf/cm^2
p_{wh} : shear reinforcement ratio in horizontal direction = a_{wh} / th_0 ,
where, a_{wh} : cross-sectional area of all horizontal rebars, h_0 : clear height of wall
σ_0 : vertical axial stress per gross horizontal area of wall, in kgf/cm^2, t : wall thickness, in cm
j : distance between compressive and tensile resultants, and may be assumed to be (7/8)d

For the specimens A-GM-F and B-GM-F, two different theoretical ultimate lateral strengths in shear failure mode (Q_{su}) are shown in Table 4, where the strength in Case 1 is determined by assuming that the wall panels of GM-F type specimens are R/C walls having effective wall thickness of 10.3 cm, while the strength in Case 2 is determined by assuming that the wall panels of GM-F type specimens are grouted masonry walls having 12.5 cm wall thickness. This effective wall thickness is determined by dividing the cross-sectional area of the grouted concrete by horizontal wall lengths (l), where the cross-sectional area of the grouted concrete is obtained by subtracting the horizontal area of all webs from the gross horizontal area of the wall.

In order to examine accuracy of the ultimate flexural and shear strengths of the grouted masonry walls predicted by the existing equations, those value were compared with the observed ultimate lateral strengths. Figure 8 shows the results of comparison for all of the A- and B-series specimens and four grouted masonry wall specimens (H- and L-series specimens) in Reference [Kikuchi et al., 1997], of which the predicted and observed ultimate lateral

strengths are shown in Table 4. H- and L-series specimens were tested in the same manner as the A- and B-series tests except that the location of applied lateral forces in H-series test, which is 1.38 of the clear height (h_0) of the wall panel measured from the bottom of the wall, is higher than that in A-, B- and L-series tests.

Comparison of the observed ultimate lateral strengths with the predicted ultimate lateral strengths for each of the specimens is shown in Figure 8. Solid symbols and open circles in Figure 8 represent the grouted masonry wall specimens and the R/C wall specimens, respectively. It can be understood from Figure 8 and Table 4 that the ultimate lateral strengths and failure modes obtained from the grouted masonry wall specimens and the R/C wall specimens can be predicted well by the existing equations, except that the observed ultimate lateral strength for specimen A-RC-190 is 19 % smaller than the predicted one.

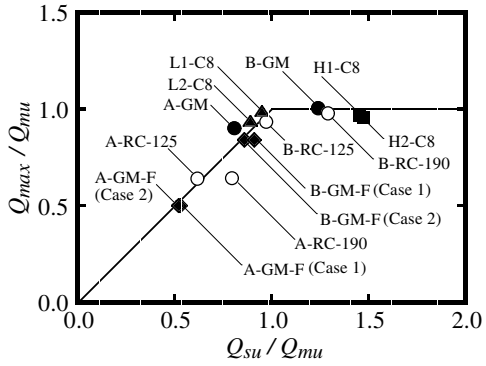

Figure 8: Comparison of the observed and predicted ultimate strengths

4.4 Components of Deformation

For measurements of shear and flexural deformation of the walls, the wall panel was divided into two segments, as shown in Figure 9, and vertical, horizontal and diagonal displacements for each segment were measured by high sensitivity displacement transducers. Using these displacement informations, flexural and shear deformation of the walls were estimated on the basis of theoretical considerations shown in Reference [Xiao et al., 1993]. The ratio of shear deformation to wall top displacement versus story drift relations obtained from all the B-series specimens are shown in Figure 10. In each curve shown in Figure 10, solid circle represents the story drifts at developing the ultimate lateral strength and open triangle represents the ultimate deformation of each specimen. The ultimate deformation is defined as the lateral displacement when the ratio of shear deformation finally begins to increase rapidly. The ultimate deformations of each specimen are also plotted in Figures 5 (e) through 5 (h). It can be understood from Figures 5 and 10 that the ultimate deformations are coincident with the story drifts at the occurrence of deterioration in lateral load-carrying capacity. In Figure 10, the ratio of shear deformation of the specimen B-GM is smaller than those of the specimens B-RC-125 and B-GM-F, and slightly larger than that of the specimen B-RC-190 generally.

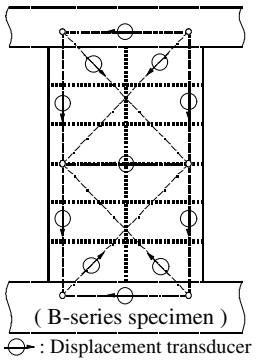

Figure 9: Arrangement of displacement transducers

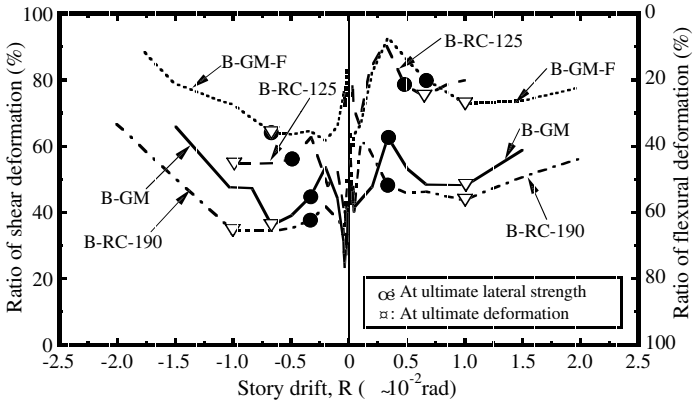

Figure 10: The ratio of shear and flexural deformations to total deformation

4.5 Principal Strains on the Surface of Walls

Relations between applied lateral force (Q) versus principal strains (ε_1 and ε_2) obtained from the specimens A-GM and A-RC-190 in the A-series test are shown in Figure 11, where the principal strains are calculated from strains measured by triaxial strain gages at the center of the surface of walls as shown in Figure 2 and are shown until developing the ultimate lateral strengths for each specimen. The principal strains occurred on the face shells of the specimen A-GM are slightly smaller than the specimen A-RC-190 under the same lateral forces. However, the principal strains in the specimen A-GM are approximately proportional to the lateral forces as well as the specimen A-RC-190. Considering this fact and crack informations, it can be understood that if the face shells and webs of the masonry units are firmly connected each other, the masonry units have an effect on confining the grouted concrete, and the face shells behave together with the grouted concrete at least until developing their ultimate lateral strengths.

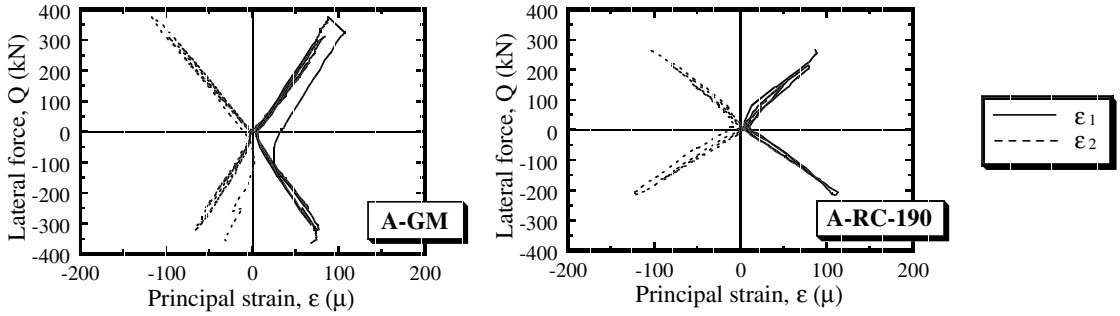

Figure 11: Lateral loads (Q) – principal strain (ε) relations

5. CONCLUSIONS

In order to investigate the effect of the presence of masonry units on the seismic behavior of reinforced fully-grouted concrete masonry walls, tests by using the eight different bearing walls including grouted masonry walls and R/C walls were conducted. In addition, accuracy of the predicted ultimate flexural and shear strengths of the grouted masonry walls by the existing equations were examined. The obtained results demonstrated the following conclusions.

1. The reinforced fully-grouted concrete masonry walls have almost the same seismic resistant capacity, such as initial stiffness, ultimate strength, deformation capacity and failure mode, as the R/C walls with the same wall thickness as the grouted masonry wall.
2. The ultimate lateral strength and the failure mode of the reinforced fully-grouted concrete masonry walls can be predicted well by the existing equations for evaluating the ultimate flexural and shear strengths of the grouted masonry walls.
3. The ratio of shear deformation of the grouted masonry wall specimen is slightly larger than that of the R/C wall specimen with the same wall thickness.
4. The masonry units have a large effect on the ultimate strength of reinforced fully-grouted concrete masonry wall.
5. The presence of webs reduces the ultimate lateral strength of the bearing wall in case when the webs of masonry units separated from face shells are located in the R/C wall.

6. REFERENCES

Architectural Institute of Japan (AIJ) (1990), *Ultimate Strength and Deformation Capacity of Buildings in Seismic Design (1990)*, pp.605-606 and 620-621, in Japanese.

Architectural Institute of Japan (AIJ) (1994), *AIJ Standards for Structural Design of Masonry Building Structures (1989 Edition)*, in English, (Spanish version is also available in CENAPRED (National Center for Disaster Prevention) in Mexico D.F., MEXICO .)

Architectural Institute of Japan (AIJ) (1997), *AIJ Standards for Structural Design of Masonry Structures (1997)*, in Japanese.

Bruneau, M. and Yoshimura, K. (1996), "Damage to masonry buildings caused by the 1995 Hyogo-ken Nanbu (Kobe, Japan) Earthquake," *Canadian Journal of Civil Engineering*, Vol. 23, No. 3, pp.797-807.

Kaminosono, T., Yamaguchi, Y. and Kawai, R. (1985), "U.S.-Japan coordinated earthquake research program on reinforced masonry buildings (6)," *Summaries of Technical Papers of Annual Meeting*, Architectural Institute of Japan, C, Structures, pp.1091-1092, in Japanese.

Kikuchi, K., Yoshimura, K., Kanema, T. and Tanaka, A. (1997), "Effect of vertical axial loads on seismic behavior of grouted masonry walls," *Proceedings of the 11th International Brick/Block Masonry Conference*, Shanghai, China, Vol. 1, pp.595-604.

Xiao, Y., Priestley, M.J.N. and Seible, F. (1993), "Steel jacket retrofit for enhancing shear strength of short rectangular reinforced concrete columns," *Report of Structural Systems Research Project*, University of California, San Diego, Report No. SSRP-92/07, pp.56-60.

Yoshimura, K., Kikuchi, K., Basaki, J., Okamoto, T. and Kai, S. (1997), "A New AIJ (Architectural Institute of Japan) Standard for Structural Design of Medium-rise Grouted Masonry Building Structures," *Proceedings of the 11th International Brick/Block Masonry Conference*, Shanghai, China, Vol. 2, pp.981-990.